Submitted to the ApJ
Preprint typeset using LaTeX style emulateapj v. 6/22/04

TYPE IA SUPERNOVA EXPLOSION: GRAVITATIONALLY CONFINED DETONATION

T. Plewa[1,2,3], A. C. Calder[1,2], and D. Q. Lamb[1,2,4]

Submitted to the ApJ

ABSTRACT

We present a new mechanism for Type Ia supernova explosions in massive white dwarfs. The proposed scenario follows from relaxing the assumption of symmetry in the model and involves a detonation created in an unconfined environment. The explosion begins with an essentially central ignition of stellar material initiating a deflagration. This deflagration results in the formation of a buoyantly-driven bubble of hot material that reaches the stellar surface at supersonic speeds. The bubble breakout forms a strong pressure wave that laterally accelerates fuel-rich outer stellar layers. This material, confined by gravity to the white dwarf, races along the stellar surface and is focused at the location opposite to the point of the bubble breakout. These streams of nuclear fuel carry enough mass and energy to trigger a detonation just above the stellar surface. The flow conditions at that moment support a detonation that will incinerate the white dwarf and result in an energetic explosion. The stellar expansion following the deflagration redistributes stellar mass in a way that ensures production of intermediate mass and iron group elements consistent with observations. The ejecta will have a strongly layered structure with a mild amount of asymmetry following from the early deflagration phase. This asymmetry, combined with the amount of stellar expansion determined by details of the evolution (principally the energetics of deflagration, timing of detonation, and structure of the progenitor), can be expected to create a family of mildly diverse Type Ia supernova explosions.

Subject headings: hydrodynamics — instabilities – stars:interior — supernovae:general — white dwarfs

1. INTRODUCTION

Type Ia supernovae are one class of luminous stellar explosions. These are the predominant explosive events in old stellar environments such as elliptical galaxies. The ejecta of these objects are rich in intermediate mass and iron group elements. Explaining the nature of these objects is therefore critical for understanding galactic chemical evolution (Truran & Cameron 1971). These supernovae also are the key component of one method used to determine the history of the Universe and probe the origin of dark energy (Sandage & Tammann 1993; Perlmutter et al. 1999; Tonry et al. 2003; Knop et al. 2003).

The work presented in this *Letter* builds on many previous observational and theoretical contributions to the field of Type Ia SNe, and on advances in fluid dynamics, nuclear physics, and computational science. Current ideas about the Type Ia supernova explosion mechanism follow from the original work of Arnett, Nomoto, and Khokhlov (Arnett 1969; Nomoto, Sugimoto, & Neo 1976; Khokhlov 1991), who pioneered deflagrating and detonating massive white dwarfs originally proposed by Hoyle & Fowler (1960) as the core component of Type Ia supernovae.

Despite decades of effort, these events remain an unsolved mystery. Proposed explosion scenarios include white dwarf detonations (Arnett 1969; Nomoto 1982), coalescing pairs of white dwarfs (Webbink 1984; Iben & Tutokov 1984), deflagrations or delayed detonations of massive white dwarfs (Nomoto, Thielemann, & Yokoi 1984; Khokhlov 1991), and collapse in a strong gravitational field (Wilson & Mathews 2004). None of these scenarios accounts for all the observed features of Type Ia supernovae. Some models produce energetic explosions but fail to explain the observed ejecta compositions, while others successfully produce the observed chemically stratified ejecta but require including ad hoc physics.

Here we report the results of multi-dimensional hydrodynamical simulations of the long-term evolution of a massive white dwarf following an essentially central ignition. The initial evolution results in a deflagration front and formation of a Rayleigh-Taylor unstable buoyancy-driven bubble that is accelerated to supersonic speeds on its way to the stellar surface. We follow the evolution beyond bubble breakout and observe formation of gravitationally confined flow across the surface of the star. The flow is focused at the point opposite the breakout location, where the matter is compressed and heated, igniting a detonation wave just above the stellar surface. We find that the star expands substantially during the evolution. This expansion produces a density distribution that, when overrun by the detonation wave, can be expected to result in ejecta that are strongly layered and rich in intermediate mass elements, as is typical of Type Ia supernovae. The modest asymmetry in the expansion of the star can also be expected to produce a mild amount of global asymmetry in the explosion.

2. NUMERICAL MODEL

The simulations presented here were performed with the adaptive mesh refinement hydrodynamics code FLASH (Fryxell et al. 2000). The numerical scheme includes self-gravity solved using a multipole expansion.

[1] Center for Astrophysical Thermonuclear Flashes, The University of Chicago, Chicago, IL 60637
[2] Department of Astronomy & Astrophysics, The University of Chicago, Chicago, IL 60637
[3] Nicolaus Copernicus Astronomical Center, Bartycka 18, 00716 Warsaw, Poland
[4] Enrico Fermi Institute, The University of Chicago, Chicago, IL 60637

We have established that to properly account for asymmetries in the mass distribution and to ensure momentum conservation in the model, at least 3 multipole moments are needed in the expansion. In the simulations reported here, we used 10 multipole moments. The rest of the physics modules are identical to those used in our previous study (Calder et al. 2004), in particular the evolution of the deflagration front is computed with a flame capturing scheme with energy release accounting for carbon, magnesium, and silicon burning (Khokhlov 2001).

The computational domain is a two-dimensional region in cylindrical geometry covering a region from $-16,384$ km to $16,384$ km in the z-direction and extending up to $16,384$ km in radius. We employed an outflow-only boundary condition at all domain boundaries, except along the symmetry axis at $r = 0$ where we used a reflecting boundary condition. The adaptive mesh was used to track flow features at a maximum effective resolution of 8 km (corresponding to an effective grid resolution of 2048×4096). The simulation was executed at Courant number of 0.6, and the time step was limited to a maximum of 4×10^{-4} s.

The initial conditions consist of a 1.36 solar mass isothermal white dwarf composed of equal amounts of carbon and oxygen with a temperature of 3×10^7 K. The progenitor model was mapped to the computational grid following the procedure employed in Calder et al. (2004). The nuclear flame was initiated as a small spherical region of completely burned material placed in hydrostatic equilibrium with its surroundings. The ignition region centered at $(r, z) = (0, 12.5)$ km had a radius of 50 km.

3. RESULTS

Figure 1 depicts several moments in the evolution of the density of the star from the point of bubble breakout to just prior to the ignition of the detonation. The rapid ascent of the bubble toward the stellar surface accelerates the stellar material located just above the bubble. This piston-like behavior results in the formation of a bulge filled with high-pressure high-momentum nuclear ash. During breakout, bubble material is expelled mostly radially, while the high pressure of the burned material accelerates the surface layers laterally (Fig. 1(a)). This material races along the stellar surface, followed by the magnesium-rich bubble material. Both remain gravitationally confined to a relatively thick ≈ 1000 km layer (Fig. 1(b)). At $t \approx 1.8$ s, this flood of surface material converges at the point opposite to the bubble breakout location, forming a conical compressed region bounded by the shock. This structure stretches down the symmetry axis beginning at $z \approx -3 \times 10^8$ cm (Fig. 1(c)).

At this point in the evolution, conditions in the shocked region approach the detonation regime. By $t = 1.85$ s, material upstream of the confluence region has density of $\approx 10^4$ g cm^{-3} and moves at velocity $9,500$ km s^{-1}. Downstream of the shock, the density of the nuclear fuel is $\approx 5 \times 10^4$ g cm^{-3} and the temperature reaches $\approx 1.4 \times 10^9$ K. Due to a mild density gradient present in the flooding material (Fig. 2(a)), the post-shock density slowly increases with time while the temperature remains relatively constant. At $t \approx 1.93$ s, the post-shock conditions are suitable for igniting the nuclear fuel: the density exceeds 1.7×10^6 g cm^{-3} and the temperature is $\approx 2.2 \times 10^9$ K. The detonation point can be seen as a slightly over-pressured region located near the symmetry axis at $(r, z) \approx (0, -3.35 \times 10^8)$ cm (Fig. 2(b)).

The detonation wave born in the region above the stellar radius will sweep through the white dwarf, which underwent a substantial evolution from the moment of the ignition of the deflagration. During its ascent, the rising bubble displaced about 5% of the stellar mass. This mass displacement, combined with the pressure wave caused by nuclear energy release, leads to expansion of the star. Thermal expansion is present from the onset of the deflagration with that part of the star nearest the deflagration experiencing relatively stronger thermal expansion. The global evolution of the stellar matter is, however, primarily in response to the softening of the gravitational potential caused by mass displacement. This expansion has a mostly radial character and becomes effective only after bubble breakout.

Figure 3 shows the evolution of density during the course of the simulation. Shown is the amount of mass in several density intervals. The material with density $> 1 \times 10^8$ g cm^{-3} will undergo burning to iron peak elements, while material with density below 3×10^7 g cm^{-3} will burn into intermediate mass elements. Several points can be noted here. There is almost no stellar expansion prior to the bubble breakout ($t \leq 0.9$ s). The breakout is followed by relatively fast expansion of the densest material ($\rho > 1 \times 10^9$ g cm^{-3}), which is succeeded by uniform expansion (identified by a simultaneous increase in the expansion rates at $t \approx 1.2$ s). This process continues until the ignition of the detonation, with the most rapid expansion at densities between 1×10^7 g cm^{-3} and 1×10^8 g cm^{-3}. At the time of detonation the amount of mass at the densities characteristic for production of intermediate mass elements, $\rho < 3 \times 10^7$ g cm^{-3}, is 0.35 $M_\odot$. The amount of mass at densities above 1×10^8 g cm^{-3}, required for production of the iron peak elements, is 0.71 $M_\odot$.

4. DISCUSSION AND CONCLUSIONS

We presented a gravitationally confined detonation (GCD) mechanism for Type Ia supernova explosions. The basic components of the proposed scenario are a rising deflagrating bubble expelling a small amount of stellar matter, the associated stellar expansion caused by the shallower potential well, the flood of stellar material across the surface following the bubble breakout, and a detonation in an gravitationally confined environment.

In the GCD scenario, not imposing any asymmetries in the initial conditions is of paramount importance. A deflagration front is born very close to the white dwarf center. Such an essentially central ignition is more probable than the idealized conditions adopted in standard deflagration or delayed detonation models, primarily because the central region of the star is convective. This type of ignition results in a rising deflagrating bubble accelerated by buoyancy to supersonic speeds on its way to the stellar surface. The transonic phase of the bubble's rise is accompanied by the formation of a bow shock ahead of the bubble that compresses and heats the nuclear fuel. Our attempts to associate this region with a possible transition to detonation failed. We discovered, however, that the flood of the expelled surface layers that follows the bubble breakout remains confined to low radii above the star. This flood races around the star and is

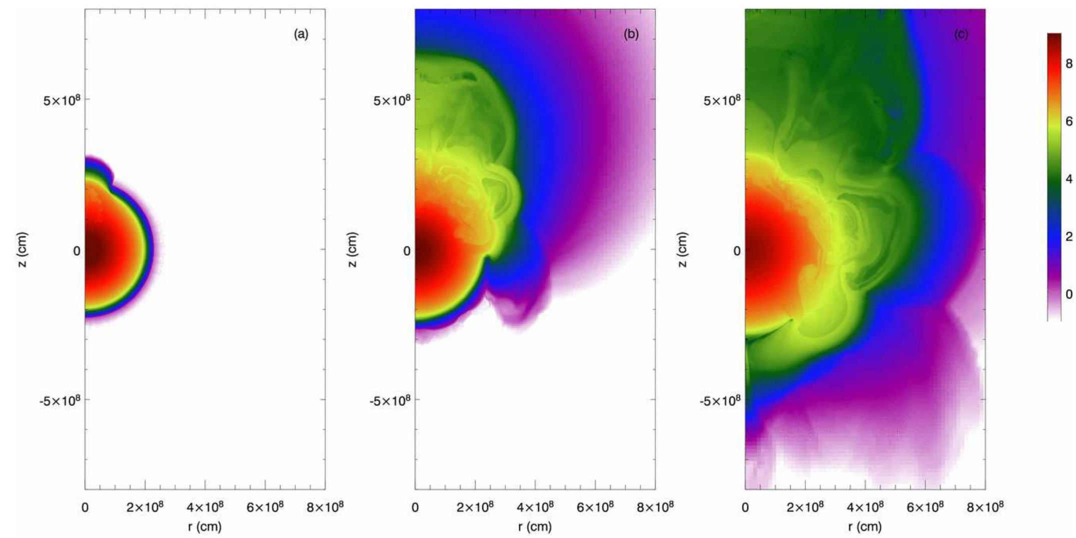

FIG. 1.— Evolution of the white dwarf following an essentially central ignition. Density in log-scale is shown for the innermost approximately one-sixth of the simulation domain. (a) The bubble breakout ($t = 0.9$ s). The material is expelled radially, and the high pressure of the burned bubble material produces a lateral acceleration of the outer layers of the star. (b) The bubble material expands above the star as the fuel-rich surface layers reach the equator in their race across the stellar surface ($t = 1.4$ s). Note that most of the surface layers are closely confined to the star. (c) Focusing of the fuel-rich streams just prior to the detonation ($t = 1.9$ s). Note the presence of the dense conical region stretching down along the symmetry axis beginning at $(r, z) = (0, -3 \times 10^8)$ cm.

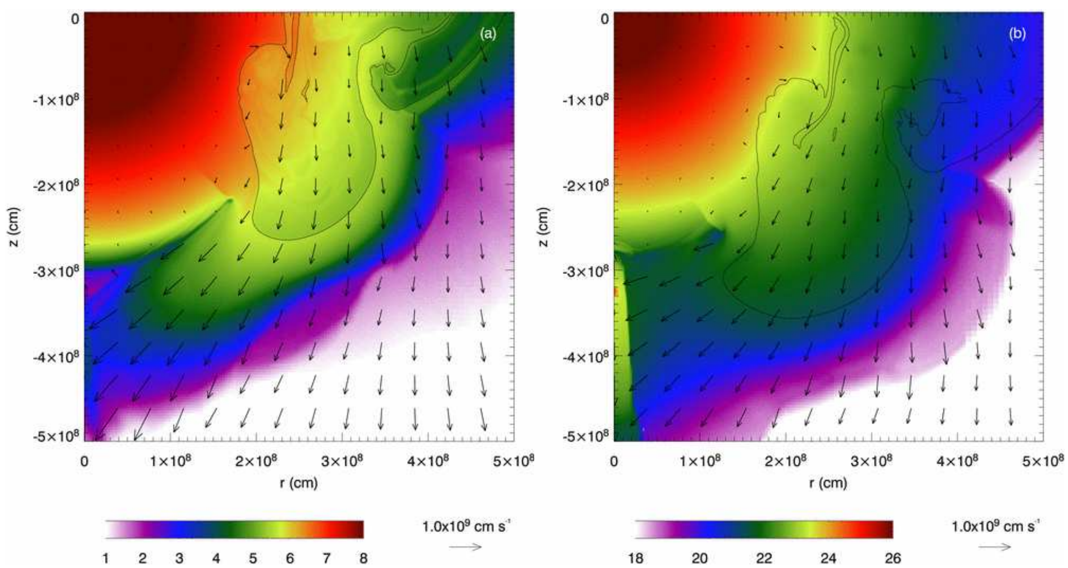

FIG. 2.— Evolution of the surface flood following an essentially central ignition of the white dwarf. The lower half of the star is shown in the figures. (a) Density in log-scale at $t = 1.85$ s. Note the density gradient present inside the stream of fast-moving material flowing across the stellar surface. Also note that the interior of the star remains highly radially symmetric, and that only relatively low-density regions are perturbed by the surface flow. (b) Pressure in log-scale at the time of the ignition of the detonation ($t = 2.005$ s). The ignition point can be seen as a small over-pressured region located near the symmetry axis at $(r, z) \approx (0, -3.25 \times 10^8)$ cm. The shock wave preceding the bubble material can also be seen in the low-density stellar layers near $(r, z) \approx (1.1 \times 10^8, -2.4 \times 10^8)$ cm. The contour marks the position of the advancing front of burned bubble material. Vectors show the velocity field; the magnitudes of these velocities can be determined by comparing the length of these vectors with the length of the fiducial vector, which corresponds to 1×10^9 cm s^{-1}.

ultimately focused into a hot, compressed, high density region located just above the stellar surface. Conditions in this region satisfy the criteria necessary for a detonation.

One important aspect of the GCD mechanism is that stellar expansion is a natural consequence of the essentially central ignition of a deflagration. The flame releases energy and displaces mass, softening the gravitational potential well leading to expansion of the star. The expansion will slow down on a time scale comparable to the sound crossing time of the white dwarf as the star tries to reach a new equilibrium. Therefore, we expect that at still later times, if not for the fact that the detonation will completely disrupt the white dwarf, the initial expansion would be followed by contraction of stellar material and the star would oscillate.

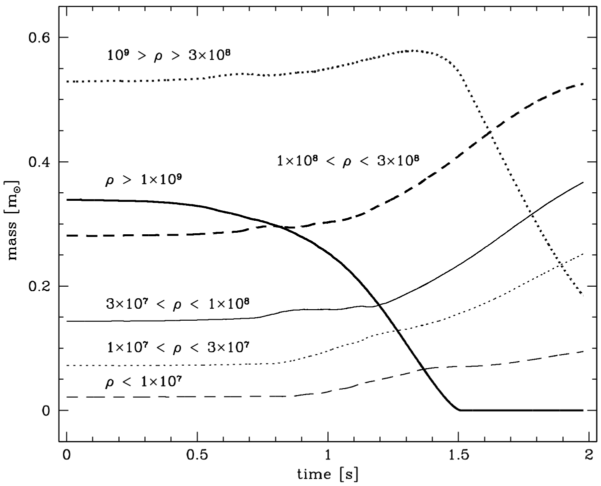

FIG. 3.— Evolution of the mass distribution in the model white dwarf. Amount of material in solar masses inside select density intervals is shown as a function of time. Significant stellar expansion takes place only after bubble breakout (about 0.9 s after the deflagration began near the center of the star). The expansion velocity increases linearly from the stellar center and leads to a steady decrease in the density of the star at all radii. At the moment of the ignition of the detonation, almost half of the stellar mass has densities below 1×10^8 g cm^{-3}.

Because of this pre-expansion, the detonation front born above the stellar surface will encounter densities similar to those found in models where pre-expansion results from a centrally ignited large-scale deflagration (Reinecke, Hillebrandt, & Niemeyer 2002; Gamezo et al. 2003). The estimate of nucleosynthetic yield for intermediate mass (iron peak) elements is a lower (upper) limit in view of the fact that the stellar expansion continues after the moment of the detonation. Determining the final yields, however, requires simulating the detonation. The actual conditions across the detonation wave, particularly the amount of compression, will influence the results. Also, the yields can be modified by delaying or by accelerating the ignition of the detonation to create a family of Type Ia supernovae with diverse spectral characteristics. The exact timing of the detonation depends on several factors. The structure of the progenitor influences energy release by the deflagration. It also affects the strength and mass of the stellar layers being pushed around the star. The radius of the progenitor regulates the time required by the streaming matter to reach the confluence point. All these factors determine the time available for stellar pre-expansion and will be a source of diversity in GCD models.

Some properties of the proposed model are, however, largely independent of the precise details of the ignition of the detonation or stellar progenitor. The explosion will be powerful. All the stellar fuel will be consumed by the detonation. Despite the perturbation introduced by the deflagration, the star will retain most of its radially symmetric stratification. Therefore, the subsequent explosion will display characteristics well-known from one-dimensional investigations (Nomoto, Thielemann, & Yokoi 1984; Höflich, Wheeler, & Thielemann 1998). In particular, we expect the distribution of nucleosynthetic products in velocity space to agree with the observed layered structure of Type Ia supernova ejecta.

The model also naturally admits certain asymmetries. The deflagration consumes only about 5% of the stellar mass. We expect a similar level of variation in the resulting spectra and luminosities, in agreement with degree of diversity present in the observations (Li et al. 2001). In addition, because the stellar shape is distorted by the rising bubble and the formation of the detonation on one side of the star, we expect a noticeable asymmetry in the stellar ejecta. These orientation effects might be responsible for peculiar events such as SN 1991T (Filippenko 1997). Because the gross properties of observed Type Ia supernovae can be accounted for in the GCD model, detailed observations will be required to verify the proposed mechanism. One possibility is to obtain information about the degree of asymmetry in these explosions, using precision polarimetric measurements.

In this short communication, we have not presented simulations that support all of our predictions. Rather, we have presented a logical sequence of events that naturally leads to a Type Ia supernova explosion. Several of these steps need to be carefully studied. In particular, the proposed detonation mechanism bears many similarities to the process of confined fusion studied in terrestrial laboratory experiments, which is notoriously difficult and prone to instabilities. For this reason, the early stages of the detonation should be studied very carefully. The expected computational demands and challenges are severe and clearly approach limits of feasibility. Despite the fact that such a study lies in the future, we are confident in the basic components of the proposed GCD mechanism.

The authors thank Alexei Khokhlov and Peter Höflich for their comments. Contributions from Natasha Vladimirova, Ed Brown, Jim Truran, and the FLASH Code Group made this work possible. This work is supported in part by the U.S. Department of Energy under Grant No. B341495 to the Center for Astrophysical Thermonuclear Flashes at the University of Chicago.

REFERENCES

Arnett, W. D. 1969, Ap&SS, 5, 180
Calder, A. C., et al 2004, ApJ Letters, submitted
Filippenko, A. V. 1997, ARA&A, 35, 309
Fryxell, B., et al. 2000, ApJS, 131, 273
Gamezo, V., et al. 2003, Science, 299, 77
Hoyle, P., & Fowler, W. A. 1960, ApJ, 132, 565
Höflich, P., Wheeler, J. C., & Thielemann, F. K. 1998, ApJ, 495, 617
Iben, I., Jr., & Tutukov, A. V. 1984, ApJS, 54, 335
Khokhlov, A. M. 1991, A&A, 245, 114
Khokhlov, A. M. 2001, ApJ, submitted (astro-ph/0008463)
Knop, R. A., et al. 2003, ApJ, 598, 102
Li, W., et al. 2001, ApJ, 546, 734
Nomoto, K. 1982, ApJ, 253, 798
Nomoto, K., Sugimoto, D., & Neo, S. 1976, Ap&SS, 39, L37
Nomoto, K., Thielemann, F.-K., & Yokoi, K. 1984, ApJ, 286, 644
Perlmutter, S., et al. 1999, ApJ, 517, 565
Reinecke, M., Hillebrandt, W., & Niemeyer, J. C. 2002, A&A, 391, 1167
Sandage, A., & Tammann, G. A. 1993, ApJ, 415, 1

Tonry, J. L., et al. 2003, ApJ, 594, 1
Truran, J. W., & Cameron, A. G. W. 1971, Ap&SS, 14, 179
Webbink, R. F. 1984, ApJ, 277, 355
Wilson, J. R., & Mathews, G. J. 2004, ApJ, in press.